

Fig. S1. Environmental predictors Oceanographic: (a) Bathymetry (m), (b) Mean temperature in the water column ($^{\circ}$ C) (c) Median velocity of current (m/s), (d) Distance to the coast and (e) Slope ($^{\circ}$); Glaciological: (f) Distance to Fourcade glacier in 2020 (m) and Sedimentological: (g) Median and (h) maximum concentration of suspended particulate matter (SPM, mg/l), and (i) mean grain size (mm). (j) Habitat age representing the time of the area free of ice rasterized from (k) glacier front lines from 1956 to 2020 was excluded from species distribution models due to high correlation with glaciological, oceanographic, sedimentological, and biogeochemical variables (Complete environmental set available in Neder 2023).

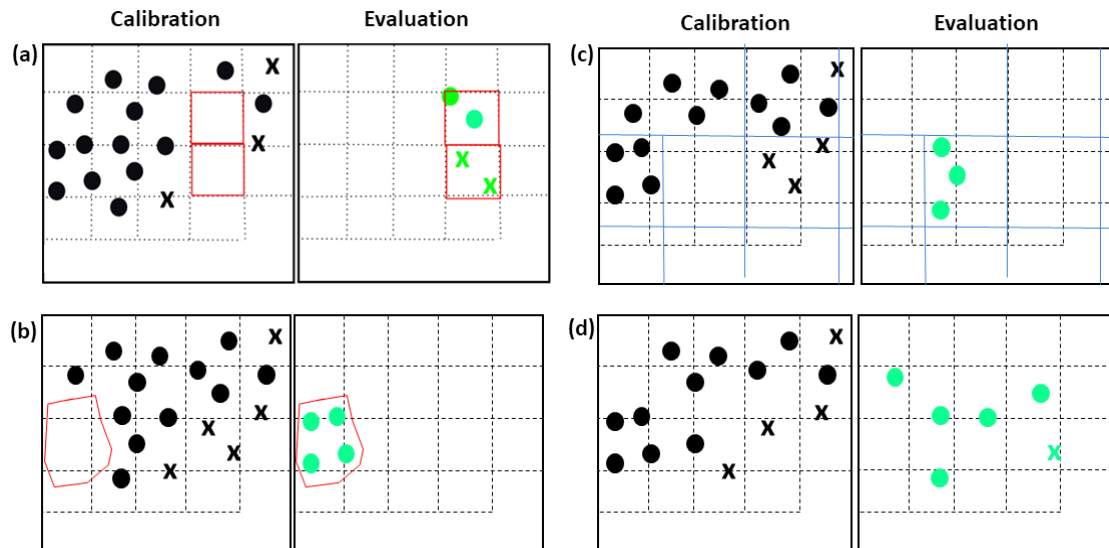


Fig. S2. Calibration: Four evaluated methods for data partitioning (in black) and evaluating species model distribution. Presence data by circles, absence by crosses. **(a)** Method 1, “blockCV” block partitioning with a size equal to the median range of spatial autocorrelation of the environmental predictors set where biological data is available. This study used this method where the pre-evaluation of 28 environmental predictors gave a median range of homogeneous environment at 1540 m without outliers. Those predictions that showed the higher spatial distance were the exposure time of ice-free area and salinity in all considered depths and mean. Further, considering only the 9 selected predictors and a median range block size of 1439 m without outliers. **(b)** Method 2, cluster partitioning by “blockCV” desired folds for cross-validation set at as default (Valavi et al. 2019). **(c)** Method 3, blocking partitioning considering latitude and longitude (line in blue) that balance presence dividing occurrences localities as equally as possible and combining ENMeval from Muscarella et al. 2014 as block calculated by the median of longitude and latitude (Guillaumot et al. 2019)¹ **(d)** Method 4, typical partitioning of 70% of presence/absence data for calibration (in black) and 30% for evaluation (in green).

Method 1 was applied for the calibration of each 30 single-model (Fig. S3). Further, the Ensemble model prediction implemented in this study goes in agreement with the “EMweight” and “pro.mean.weight” & “prob.mean.weight.decay” functions from *biomod2*. Regarding the package description, the equation computes the weighted mean of predictions from individual models, where each prediction is multiplied by its corresponding weight and then summed. The result is divided by the sum of weights to ensure the final prediction is appropriately scaled.

The equation for EMwmean can be expressed as follows:

$$EMwmean = \frac{\sum_{i=1}^n w_i \times p_i}{\sum_{i=1}^n w_i}$$

Where: *EMwmean* represents the Ensemble Model weighted mean, *n* is the number of individual models *w(i)* is the weight assigned to (*i*) each single model. Values are awarded for each method proportionally to their evaluation scores and are available from the function BIOMOD_Modeling; *p (i)* is the probability or prediction produced by (*i*) each single model. This equation calculates the weighted mean of predictions from individual models, where each prediction is multiplied by its corresponding weight and then summed (Thuiller et al. 2021; Marmion et al. 2009). The resulting sum is divided by the sum of weights to ensure the final prediction is properly scaled. Further explanations and implementations are available in R documentation “biomod2” and GitHub explanations.

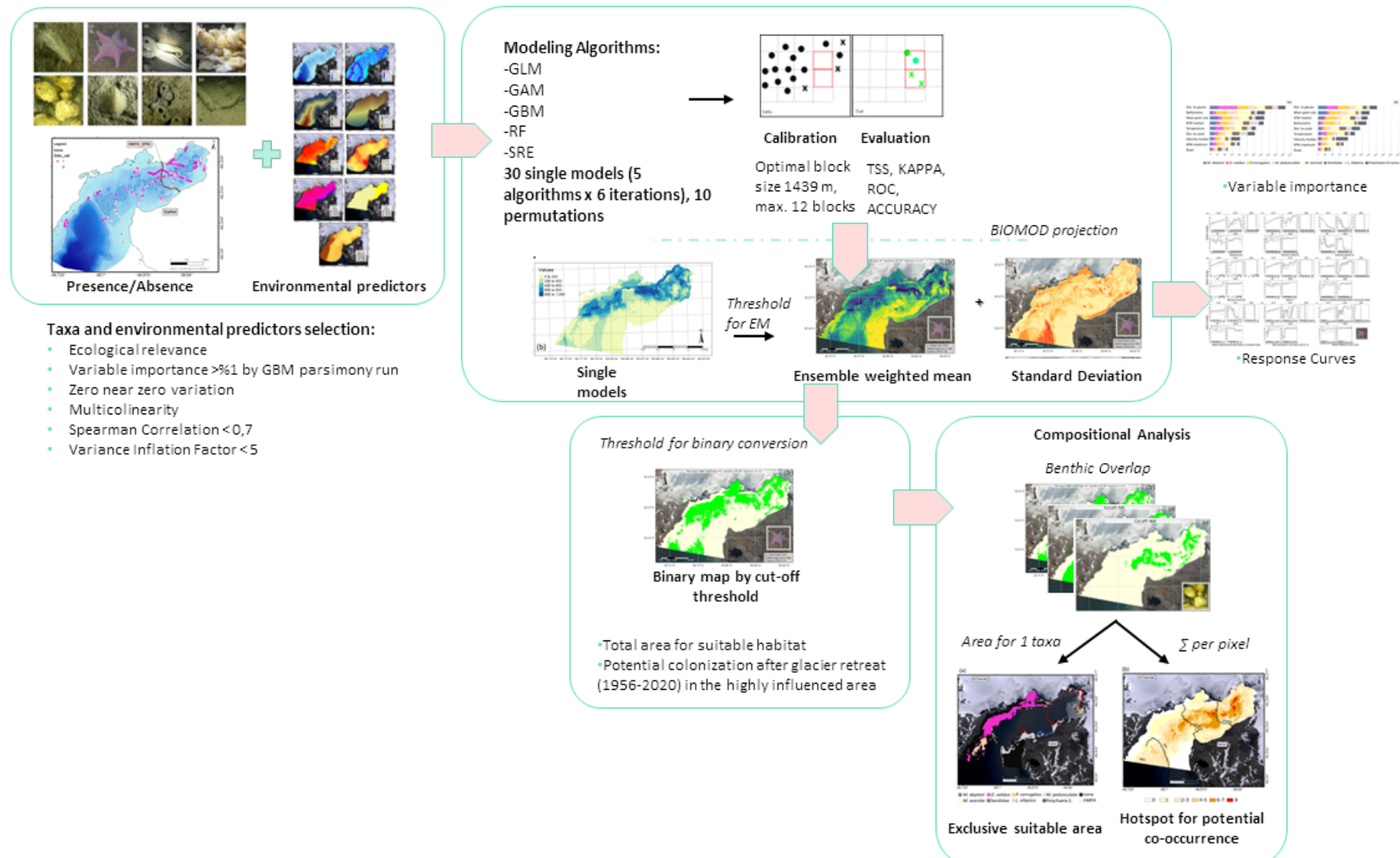


Fig. S3. Methods workflow for benthic taxa distribution model by ensemble model and post-processing analysis of binary transformation and compositional analysis (Neder & Pehlke 2024).

Table S1a. Summary of spatially modeled and interpolated oceanographic and morphological environmental variables in raster or polyline format for Potter Cove, applied as predictors in species distribution modeling (SDMs) of benthic taxa. Continued in Table S1b.

Acronym	Description	Original Raster Name	Sample year	U	Data	V	Model characteristics
bathy	Bathymetry	bathy_v2020_pc clip de bathy_raw_UKHO_Tos_TopoToRaster3d	2012	m	Jerosch et al. (2015), licencia de Open Government Licence v2.0 por United Kingdom Hydrographic Office (UKHO)	v2020	Topo to raster 3d tool in ArcGIS Pro 2.4.0. Original multibeam data. The analysis was configured with the following characteristics: arcpy.TopoToRaster3d: 'in_topo_features' = bathy_raw_UKHO_Tos como depth PointElevation; coastline2020_KGI_landsat8CN_depth como profundidad Contour, 'cell_size': 5, 'extensión': 409503,0167-3095186,095; 415009,2658-3100311,9283; Márgeas: 'min_z_value'= 20, 'max_z_value'=0; 'enforce'=NO_ENFORCE, 'data_type'=SPOT, 'max_iterations'=20, 'roughness_penalty'=default, 'discrete_error_factor'=1, 'vertical_standard_error'=0, 'tolerance_1'=0, 'tolerance_2'=1; 'out_stream_feature's=default, 'out_sink_features'=default, 'out_diagnostic_file'=default, 'out_parameter_file'=defaults, 'profile_penalty'=default, 'out_residual_feature'=default, 'out_stream_cliff_error_feature'=default, 'out_contour_error_feature'=default, 'Mask'=coastline_2020_KGI_landsat8CN_PolygonTemplate_TopotoRaster
Slope	Slope	Slope_v2020_pc clip de bathy_BTM_Slope3d_2020_v01	2012	[°]	Jerosch et al. (2015), licencia de Open Government Licence v2.0 por United Kingdom Hydrographic Office (UKHO)	v2020	Slope processed with the 'Calculate Slope' tool of 'Benthic Terrain Modeller' (Wright et al. 2012) with ArcGIS Pro 2.4.0, Configuration: 'in_topo_features'=bathy_raw_UKHO_Tos_TopoToRaster3d with the same pixel size as bathymetry: 5*5m. Input parameters: 'Elevation Raster': bathy_proc_toso_ukho_coastnew; 'Elevation Units': Meters; 'Elevation Projection': WGS_1984_UTM_Zone_21S; 'Elevation X/Y Units': Meter. 'min range': 0-15 raster cells (0-75m), 'max range': 15-250 raster cells (75-1250m)
DistCoast	Distance to coast	DistanceToCoast_v2020_pc clip of DistanceToCoast_2020_07_EuclideanDistance_Mask_withIsle	2020	m	Neder (2023); DigitalGlobe (2014), U.S. Geological Survey (2019)	v2022	Euclidean distance was performed with the 'Spatial Analyst' tool in ArcGIS 10.8.1. The analysis was configured with the following characteristics: arcpy.EuclideanDistance: 'in_topo_features'=KGI_coast_2020 with the islands considered, 'output cell size'=5m, 'distance method': geodesic. 'Mask extension': 410027,164400-415009,265792; 3100311,928285-3096344,498179
vel_med	Median water circulation velocity in summer	vel_med_nco_EPSG32721	2010/2011	m/s	Neder et al. (2022); Falk et al., (2016), (2018a), (2018b); Falk & Silva-Busso (2021); Monien et al. (2017)	v2021	FESOM-C hydrodynamic model (Androsov et al. 2019), Mean/maximum/min calculation for a typical summer (December–February). Barotropical 2D runs (depth-averaged solutions) with tidal and wind forcing. The TPXO 9 atlas was used for open boundary conditions of tidal elevation with nine different harmonic constituents. Atmospheric data derived from the CCLM 5.0 model. Glacier discharge was considered to calculate the inflow volume of each glacier sub-basin. For more information on model calculations and analysis, see the associated reference in Neder et al. (2022).
Temp_mly3	Average temperature in the stratified water column	temp_mly3	2010-2015	°C	Neder et al. (2017) & associated in Pangaea	v2022	Temperatura media de la columna de agua ponderada por la profundidad. El cálculo consiste en la utilización de la herramienta "raster calculator" (ArcGIS 10.8.1) donde a profundidades menores a 5 m, el valor de la temperatura está dado por aquel interpolado en la capa 1-5 m, mientras a profundidades entre 5-15 m por el promedio de la capas 1-5m y 5-15m, y a profundidades mayores de 15m por el promedio de las tres capas del ráster de 1 a 5 m, de 5 a 15 m y de más de 15 m.

Table S1b. (Continuation). Summary of spatially modeled and interpolated glaciological and sedimentological environmental variables in raster or polyline format for Potter Cove, applied as predictors in species distribution modeling (SDMs) of benthic taxa. Added the time of ice-free as an explanatory variable of spatial distribution.

Acronym	Description	Original Raster Name	Sample year	U	Data	V	Model characteristics
DistGlac	Distance to Glacier Front 2020	DistanceToGlacier_v2020_pc clip de DistanceToGlacier_2020_07_Euclidean Distance	2020	m	Neder (2023); DigitalGlobe (2014), U.S. Geological Survey (2019)	v2020	Euclidean distance was performed with the 'Spatial Analyst' tool in ArcGIS Pro 2.4.0. The analysis was configured with the following characteristics: arcpy. EuclideanDistance: 'in_topo_features'=glacier_front_KGI_2020_combine_UTM_21S, 'output cell size'=5m, 'distance method': planar, 'extent'=408543.7374; 3094054,8273; 420601,8151; 3100566.9841, 'in_mas k_features'=Template_Polygon_PC
mgs	Mean grain size	mgs_idw_r_pc	2009;2010/2011	mm	Wölfel et al. (2013, 2014) and Sahade et al. (2015) OE2 station analysed in Neder (2023)	v2021	Inverse Distance Weighted best model calculated with R and run with ArcGIS Geostatistical Analyst (ArcGIS 10.8.1). Stations: 137 'Power' 1; 4-4 'neighbours': 1 full sector, default range (1287.172235); 5x5 resolution. Average error: -0.04275502893943323; Root mean square: 1.8177850224151066; Regression Function: 0.86158096222457 * x + 0.0345465148452702
spm_max	Maximum suspended particulate matter concentration in the summer	spm_max_nco_EPSG32721	2010/2011	mg/l	Neder et al. (2016a, 2022); Monien et al. (2017)	v2021	FESOM-C hydrodynamic model (Androsov et al. 2019), Calculation of mean/maximum/min for a typical summer (December–February). 2D barotropic runs (depth-averaged solutions) with tidal and wind forcing, parameters attributed to the sediment module such as 4.5×10^{-5} m SPM diameter size, 1450 kg/m ³ SPM density; sedimentation rate of 100% and average SPM scenario of 1.35 mg/l discharge through the glacier. The coefficient of friction of the bottom was set at 2.6×10^{-3} . For more information on model calculations and analysis, see the associated reference in Neder et al. (2022).
spm_med	Median suspended particulate matter concentration in the summer	spm_med_nco_EPSG32721	2010/2011	mg/l		v2021	
Time_icefree	Time of an area free of ice. Exposure time	Expo_icefree	1956, 1988, 1995, 2000, 2005, 2008, 2010, 2014, 2016, 2018, 2020	year	Neder (2023)	v2022	It was calculated using the raster result of the Euclidean distances to each year, then summed those rasters with the raster calculator tool, clipped the sum layer by year, e.g. 1988_1955, reclassified using the 'slice/reclassify' tool to divide the distance into equal interval/area ratio of the years of retreat and determine the ice-free exposure time (example in 7 for the ice-free area). between 1988 and 1955)

Table S2. Range of environmental variability for the presence of eight zoobenthic taxa representative of Potter Cove assemblage. For the explanation of the acronyms and the units please refer to Table S1.

Var/spp zoobenthos	Mal_day	Odo_val	Parb_cor	Mol_ped	Myc_ace	Sero	Lat_elli	Polych_Esp
bathy	3,67 - 45,95	3,67 - 47,95	3,67 - 51,98	0,94 - 51,98	3,67 - 45,82	3,67 - 45,92	3,67 - 45,92	10,86 - 51,98
BPI_broad	-22 - 47	-21 - 66	-21 - 51	-22 - 51	-21 - 46	-22 - 55	-22 - 60	-21 - 22
BPI_fine	-8 - 8	-8 - 17	-5 - 15	-8 - 17	-8 - 17	-5 - 7	-5 - 9	-5 - 11
bs_max	0,01 - 1,93	0,01 - 2,09	0,02 - 1,93	0,02 - 5,07	0,02 - 1,33	0,02 - 2,09	0,01 - 2,09	0,02 - 1,39
bs_mean	0,012 - 1,928	0,005 - 2,093	0,019 - 1,928	0,018 - 5,065	0,019 - 1,327	0,015 - 2,093	0,012 - 2,093	0,019 - 1,393
bs_med	0,001 - 0,401	0,000 - 0,401	0,001 - 0,401	0,001 - 0,401	0,002 - 0,156	0,001 - 0,114	0,001 - 0,401	0,001 - 0,092
bs_min	0,000 - 0,368	0,000 - 0,368	0,000 - 0,368	0,000 - 0,368	0,001 - 0,126	0,000 - 0,068	0,000 - 0,368	0,000 - 0,064
DistToCoast	28 - 703	0 - 831	0 - 842	0 - 843	0 - 691	28 - 814	28 - 819	7 - 841
DistToGlacier	38 - 1994	28 - 2239	32 - 2202	32 - 1752	35 - 1994	40 - 1994	29 - 1994	36 - 1480
expo_icefr	16 - 304	22 - 216	16 - 318	13 - 284	22 - 304	42 - 386	30 - 374	16 - 318
Fe2O3_02cm	7,53 - 8,91	7,32 - 8,90	7,57 - 8,88	7,55 - 8,91	7,53 - 8,89	7,37 - 8,91	7,43 - 8,91	7,60 - 8,90
Fe2O3_12cm	7,61 - 8,98	7,59 - 8,98	7,65 - 8,95	7,62 - 8,98	7,65 - 8,95	7,59 - 8,98	7,62 - 8,98	7,68 - 8,98
hydro_TAU_mi	0,001 - 0,115	0,001 - 0,165	0,001 - 0,144	0,001 - 0,106	0,001 - 0,115	0,001 - 0,115	0,001 - 0,115	0,001 - 0,012
hydro_TAU_mo	0,004 - 0,275	0,002 - 0,391	0,001 - 0,344	0,001 - 0,239	0,004 - 0,275	0,002 - 0,275	0,001 - 0,275	0,003 - 0,043
hydro_TAU_r	0,008 - 0,550	0,003 - 0,825	0,000 - 0,716	0,000 - 0,473	0,009 - 0,550	0,001 - 0,550	0,000 - 0,550	0,009 - 0,103
mgs	0,01 - 8,85	0,01 - 15,64	0,01 - 13,68	0,01 - 14,72	0,01 - 0,18	0,01 - 15,40	0,01 - 14,72	0,01 - 0,11
ProbHardS	0-1	0 - 1	0 - 1	0 - 1	0-1	0 - 1	0 - 1	0 - 1
Sal_1to5m	33,38 - 33,82	33,38 - 33,87	33,39 - 33,86	33,38 - 33,86	33,40 - 33,82	33,38 - 33,85	33,38 - 33,86	33,38 - 33,82
Sal_Sto15m	33,91 - 34,01	33,91 - 34,04	33,92 - 34,04	33,91 - 34,04	33,92 - 34,01	33,91 - 34,04	33,91 - 34,04	33,91 - 34,01
Sal_deeper15	34,04 - 34,10	34,04 - 34,12	34,04 - 34,12	34,04 - 34,12	34,04 - 34,10	34,04 - 34,12	34,04 - 34,12	34,04 - 34,11
Sal_mean_ly3	33,78 - 33,97	33,78 - 34,01	33,78 - 34,01	33,78 - 34,01	33,79 - 33,97	33,78 - 34,01	33,78 - 34,01	33,78 - 33,97
Sal_mly3	33,53 - 33,98	33,67 - 33,98	33,67 - 34,01	33,42 - 33,98	33,67 - 33,98	33,53 - 34,01	33,53 - 34,01	33,53 - 33,98
Sediments_Folk	sandy-mud / clay							
Sediments_Shephard	sandy-silt / clayey-silt							
SiO2_02cm	52,34 - 54,09	52,34 - 54,14	52,51 - 53,97	52,33 - 53,98	52,51 - 54,09	52,32 - 54,13	52,34 - 54,13	52,34 - 53,96
SiO2_12cm	52,25 - 55,88	52,16 - 56,09	52,18 - 55,55	52,16 - 55,88	52,17 - 55,57	52,25 - 55,97	52,25 - 55,81	52,16 - 55,75
Slope	0,00 - 29,97	0,00 - 45,99	0,01 - 42,99	0,00 - 45,99	0,00 - 42,99	0,00 - 27,05	0,00 - 30,78	0,00 - 41,62
spm_max	145,15 - 694,24	124,69 - 694,24	138,80 - 567,93	158,16 - 694,24	154,84 - 691,44	154,84 - 694,24	154,84 - 694,24	169,11 - 694,24
spm_mean	6,11 - 74,96	4,76 - 74,96	4,43 - 55,33	6,95 - 74,96	6,11 - 74,96	4,28 - 74,27	4,22 - 74,27	6,71 - 74,96
spm_med	0,02 - 43,02	0,00 - 43,02	0,00 - 29,21	0,23 - 43,02	0,02 - 43,02	0,02 - 37,89	0,02 - 39,68	0,82 - 43,02
spm_min	0,00 - 0,005	0,00 - 0,005	0,00 - 0,001	0,00 - 0,005	0,00 - 0,005	0,00 - 0,004	0,00 - 0,004	0,00 - 0,005
Temp_1to5m	1,24 - 1,69	1,25 - 1,78	1,25 - 1,77	1,24 - 1,56	1,25 - 1,69	1,24 - 1,69	1,24 - 1,69	1,25 - 1,56
Temp_5to15m	1,10 - 1,45	1,10 - 1,52	1,10 - 1,51	1,10 - 1,31	1,10 - 1,45	1,10 - 1,45	1,10 - 1,45	1,10 - 1,31
Temp_deeper15m	0,93 - 1,12	0,94 - 1,20	0,93 - 1,19	0,93 - 1,12	0,94 - 1,12	0,93 - 1,12	0,93 - 1,12	0,93 - 1,12
Temp_ly3	1,09 - 1,69	1,10 - 1,69	1,10 - 1,69	1,09 - 1,34	1,13 - 1,69	1,09 - 1,69	1,09 - 1,69	1,09 - 1,33
Temp_mean_ly3	1,09 - 1,42	1,10 - 1,50	1,09 - 1,49	1,09 - 1,33	1,10 - 1,42	1,09 - 1,42	1,09 - 1,42	1,09 - 1,33
vel_max	0,063 - 0,814	0,042 - 0,819	0,088 - 0,797	0,076 - 1,269	0,080 - 0,662	0,076 - 0,819	0,063 - 0,819	0,000 - 0,022
vel_mean	0,012 - 0,316	0,011 - 0,316	0,015 - 0,316	0,014 - 0,316	0,020 - 0,196	0,013 - 0,153	0,012 - 0,316	0,016 - 0,144
vel_med	0,010 - 0,345	0,009 - 0,345	0,011 - 0,345	0,011 - 0,345	0,014 - 0,198	0,010 - 0,143	0,009 - 0,345	0,012 - 0,135
vel_min	0,000 - 0,024	0,000 - 0,024	0,000 - 0,014	0,000 - 0,024	0,000 - 0,022	0,000 - 0,014	0,000 - 0,024	0,000 - 0,024

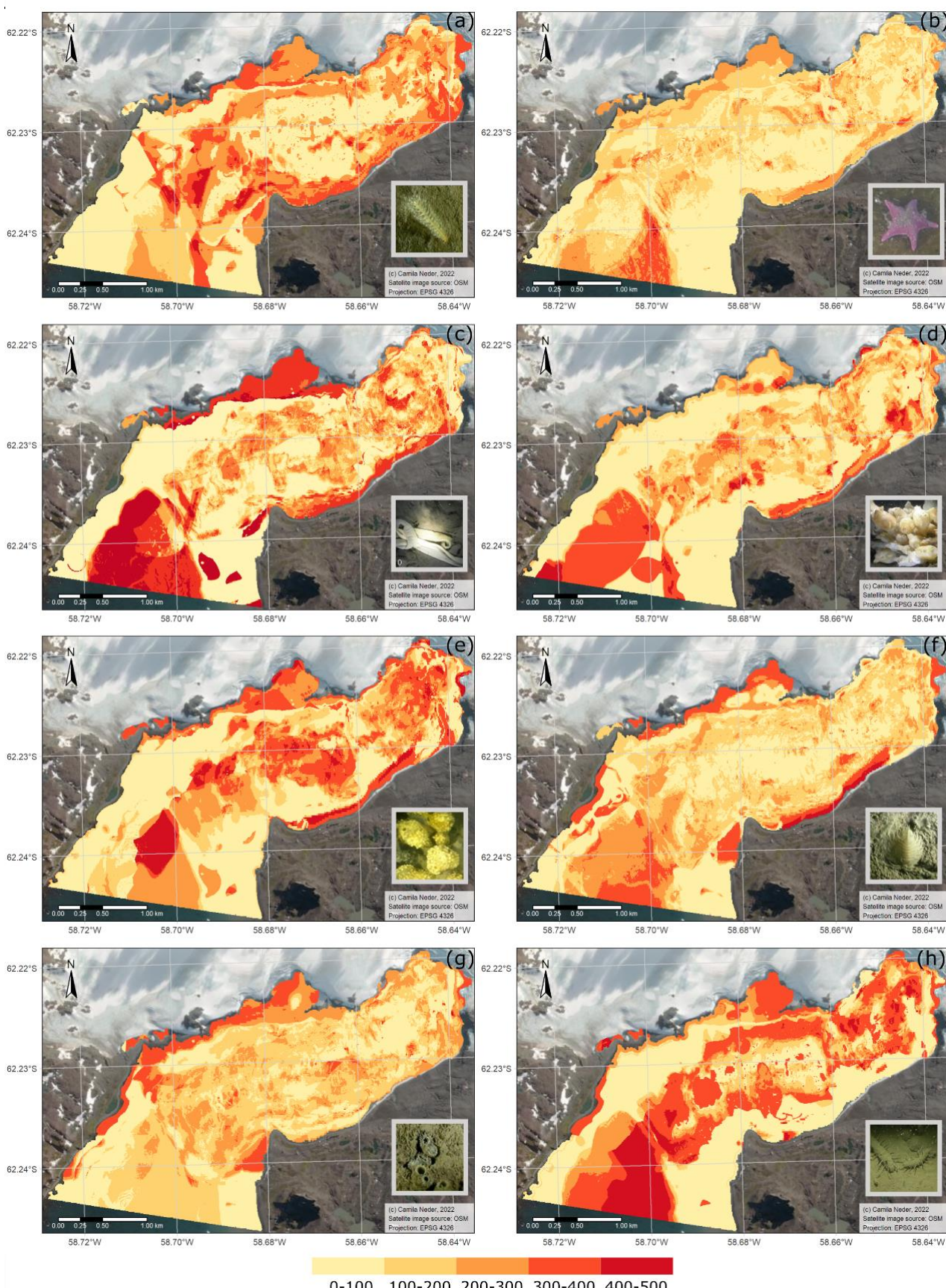


Fig. S4. Standard deviation of all models included in ensemble models. **(a)** *Malacobellemn daytoni*. **(b)** *Odontaster validus*. **(b)** *Parborlasia corrugatus*. **(d)** *Molgula pedunculata*. **(e)** *Mycale acerata*. **(f)** *Serolidae*. **(g)** *Laternula elliptica*. **(h)** Polychaeta subclass Errantia (morpho sp1).

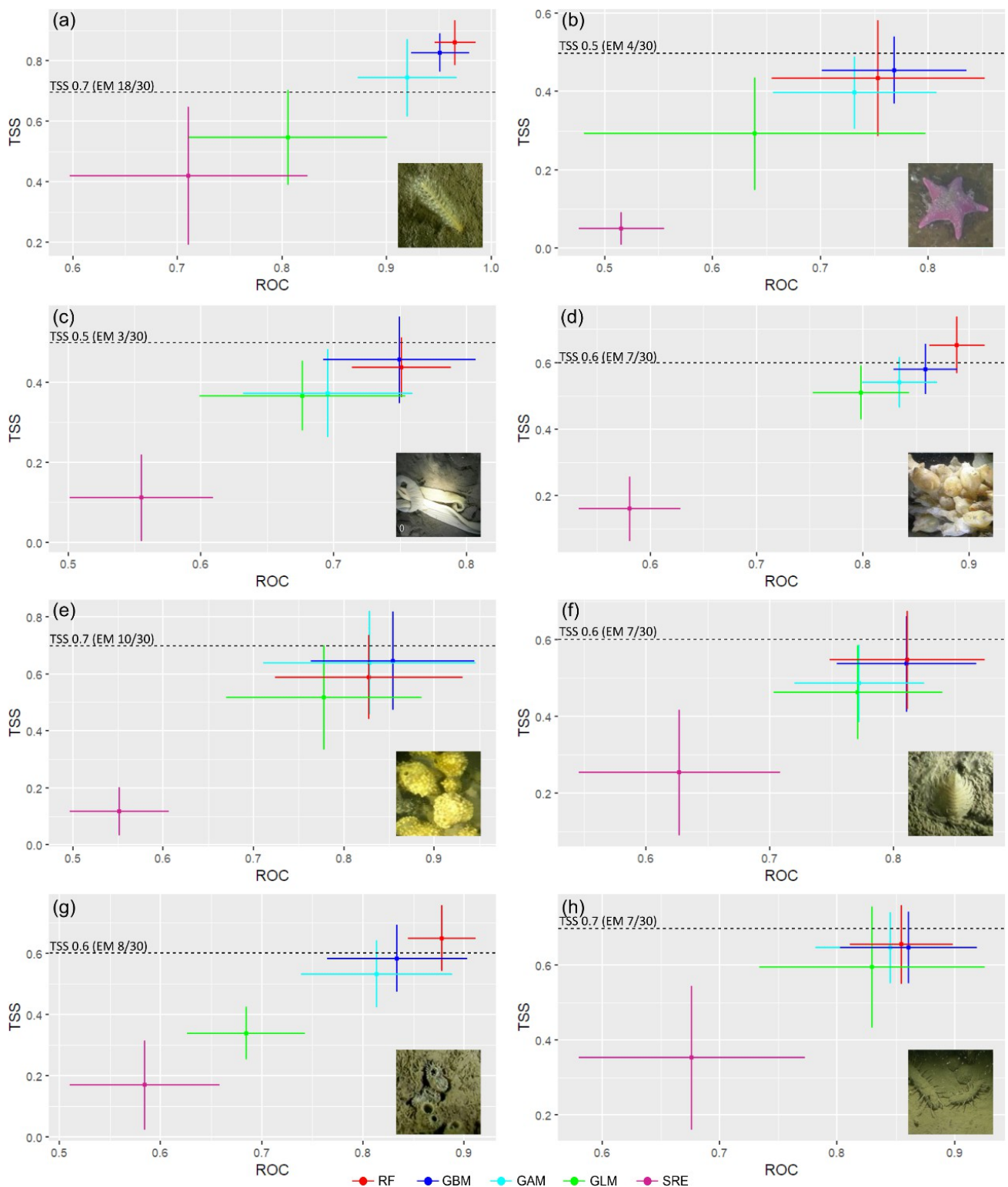


Fig. S5. Evaluation metrics of 'True Statistic Skills' (TSS) and 'Relative Operating Characteristic' (ROC) for analyzed zoobenthic taxa
(a) Pennatulid *Malacobellemnion daytoni*. **(b)** Sea star *Odontaster validus*. **(c)** Nematode *Parborlasia corrugatus*. **(d)** Ascidian *Molgula pedunculata*. **(e)** Sponge *Mycale acerata*. **(f)** Isopoda Serolidae **(g)** Bivalve *Laternula elliptica*. **(h)** Polychaeta Errantia non-identified species. The slashed line shows the TSS threshold to build the ensemble model (EM). Note the different graph scales of each taxon.

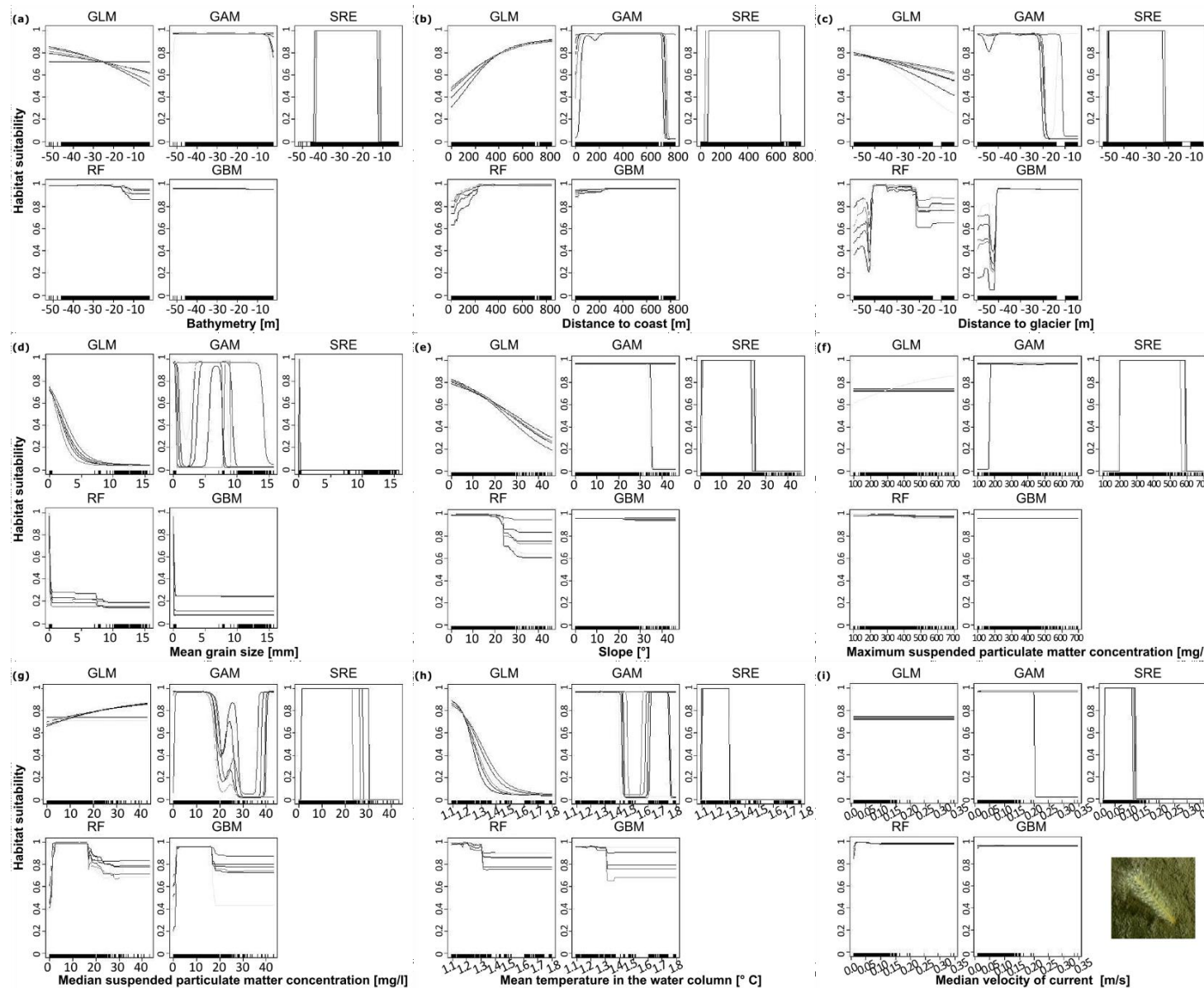


Fig. S6.1. Response curves of habitat suitability (measured as a probability of occurrence from 0 to 1) of *Malacobellemnoides daytoni* for the nine environmental selected predictors for taxa distribution modeling.

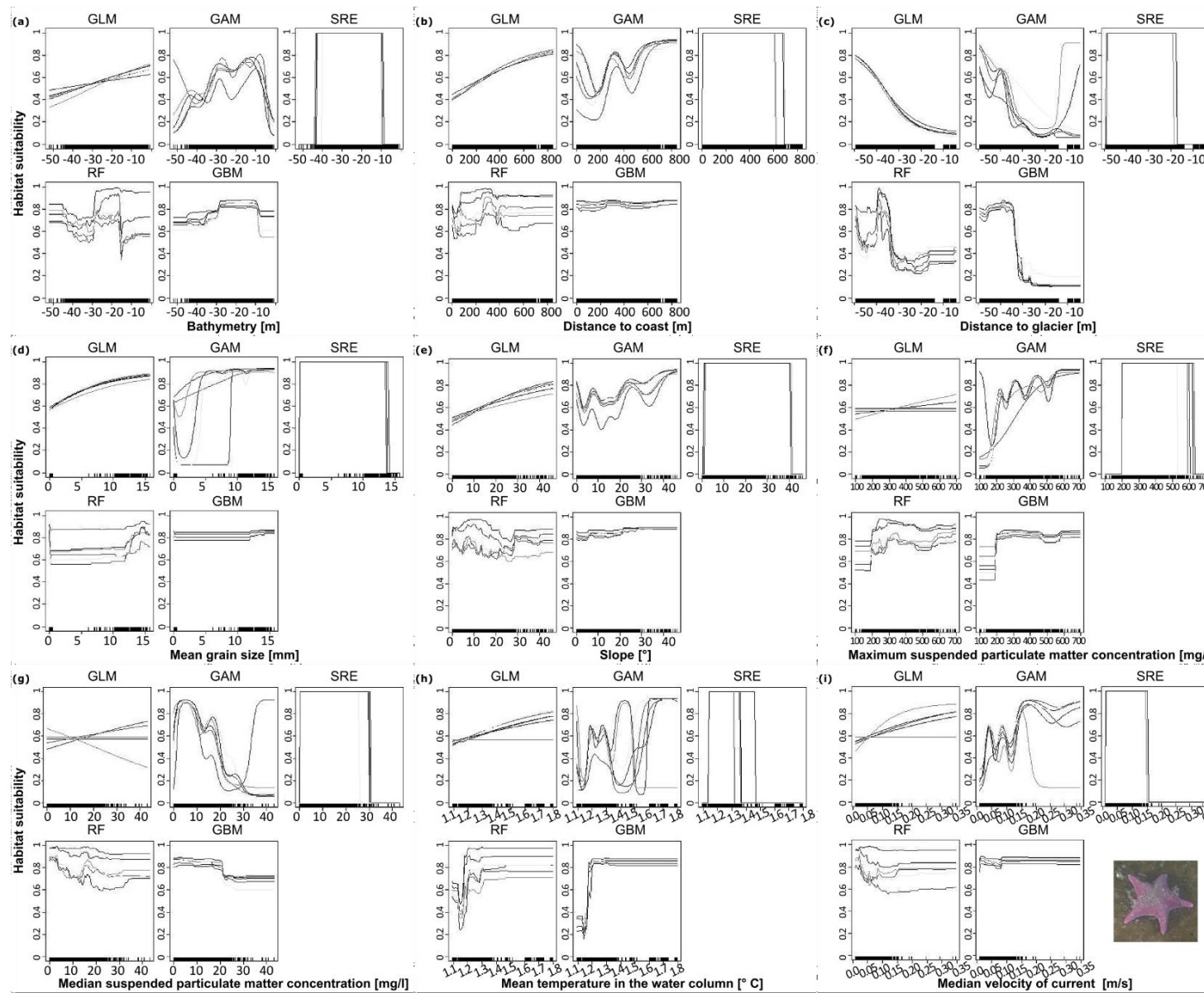


Fig. S6.2. Response curves of habitat suitability (measured as a probability of occurrence from 0 to 1) of *Odontaster validus* for the nine environmental selected predictors for taxa.

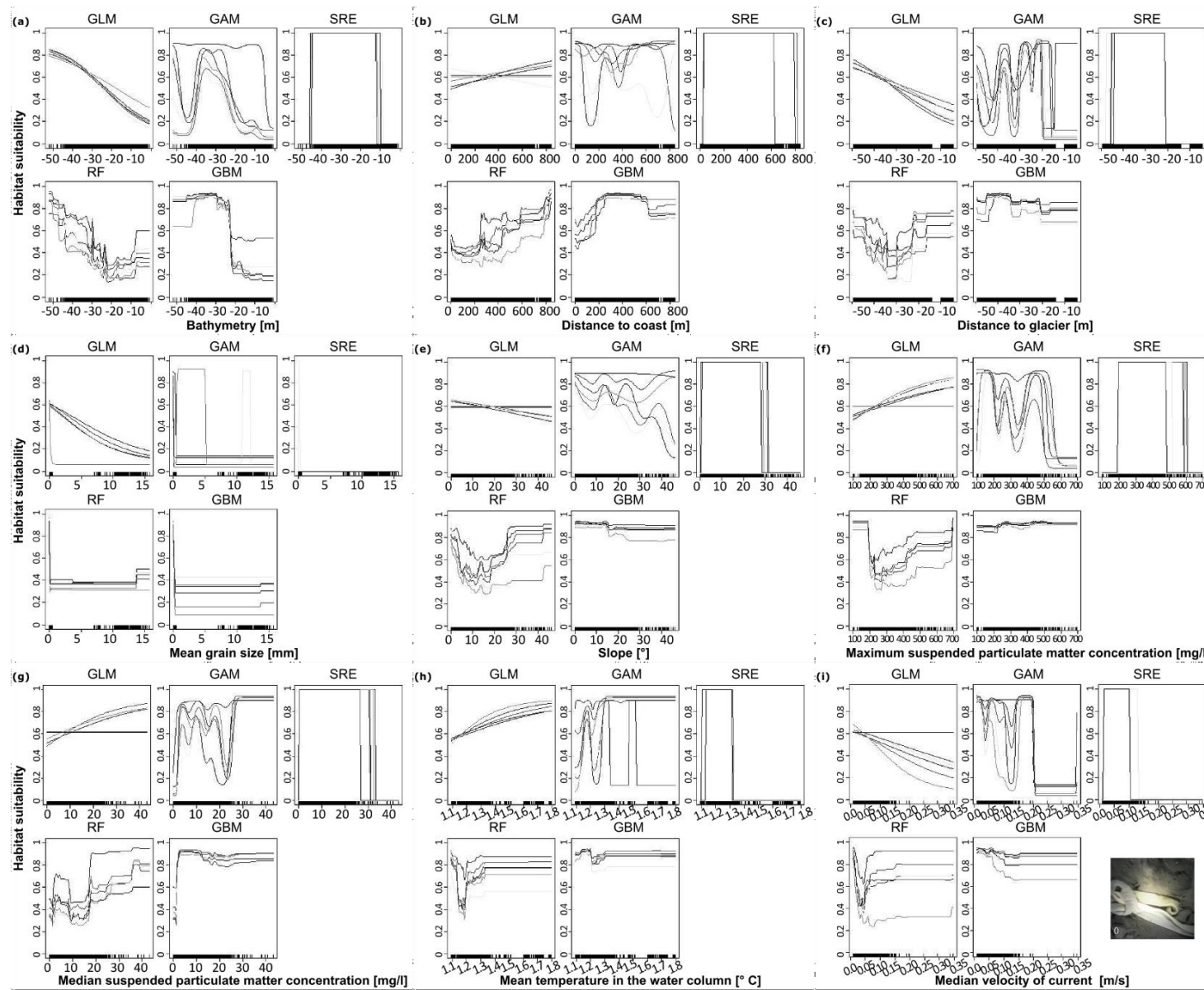


Fig. S6.3. Response curves of habitat suitability (measured as a probability of occurrence from 0 to 1) of *Parborlasia corrugatus* for the nine environmental selected predictors for taxa.

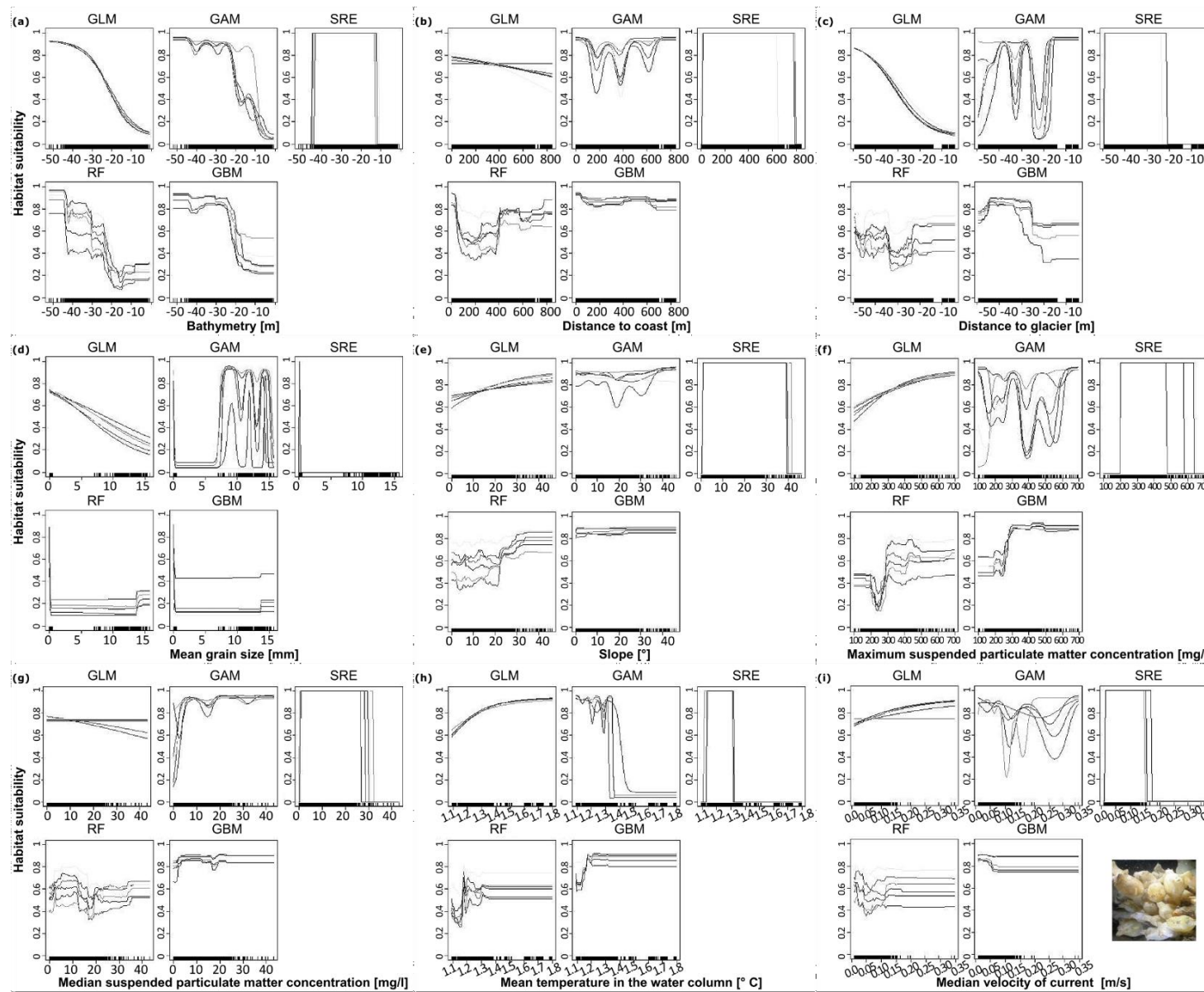


Fig. S6.4. Response curves of habitat suitability (measured as a probability of occurrence from 0 to 1) of *Molgula pedunculata* for the nine environmental selected predictors for taxa.

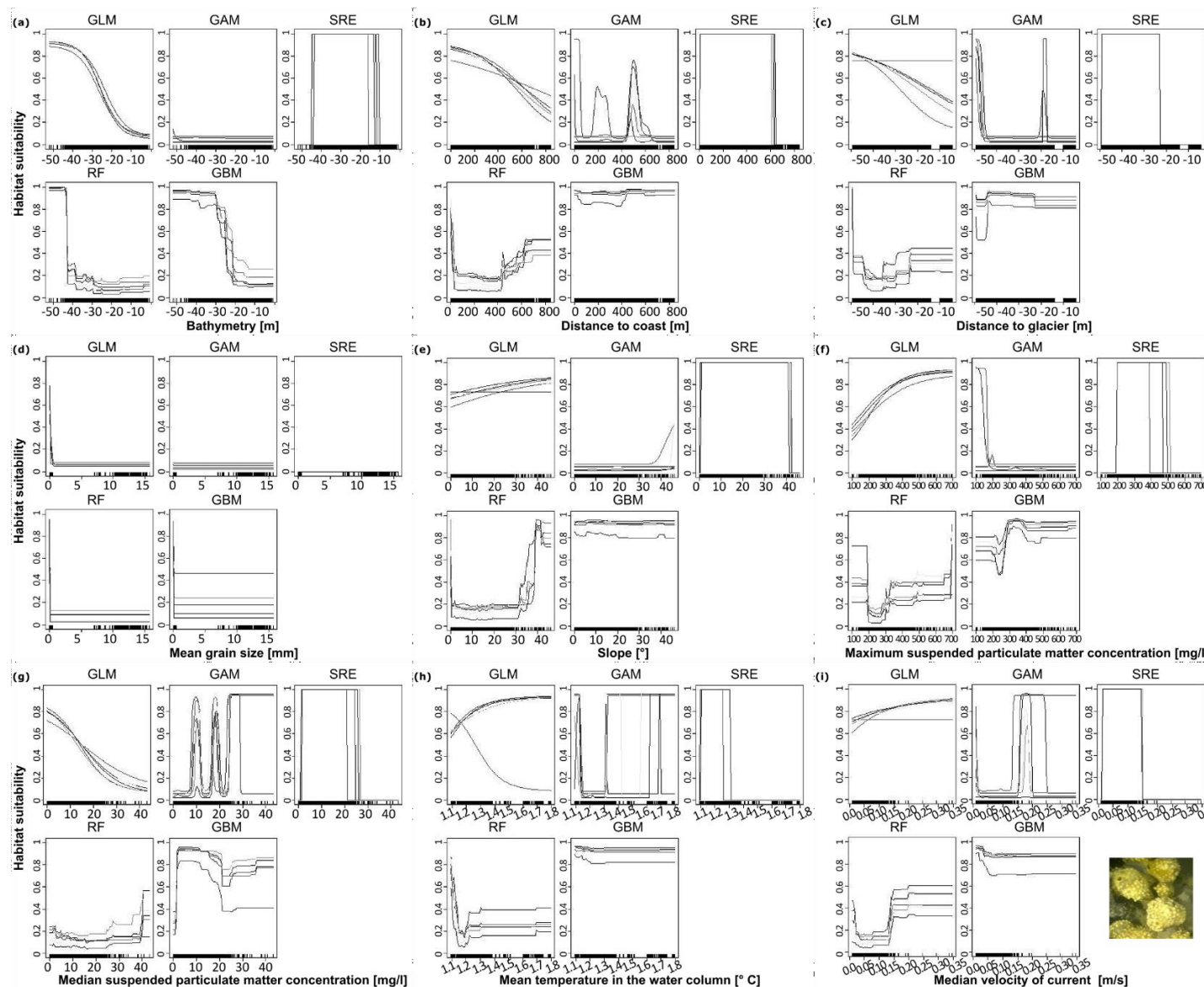


Fig. S6.5. Response curves of habitat suitability (measured as a probability of occurrence from 0 to 1) of *Mycale acerata* for the nine environmental selected predictors for taxa distribution modeling.

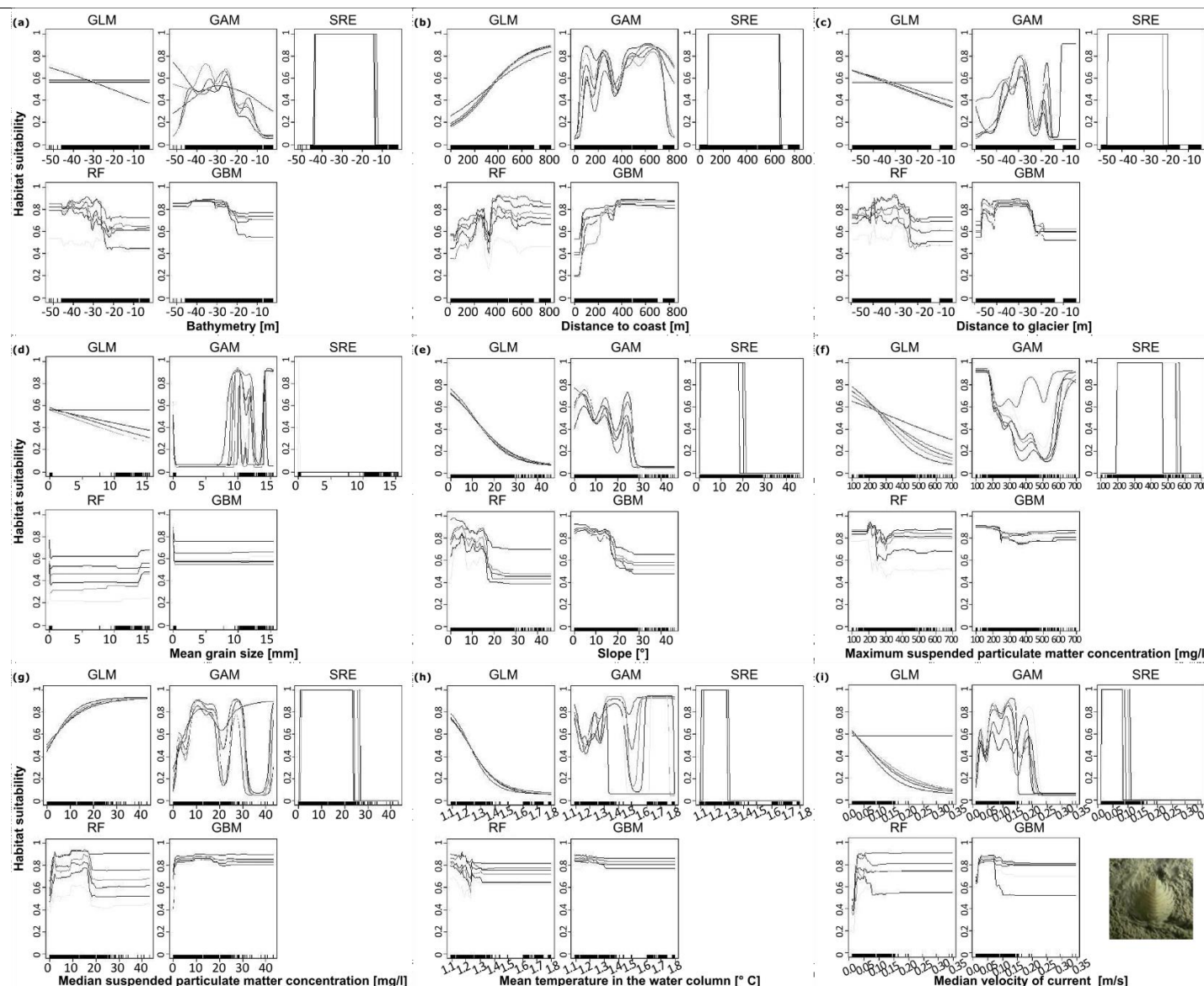


Fig. S6.6. Response curves of habitat suitability (measured as a probability of occurrence from 0 to 1) of Serolidae for the nine environmental selected predictors for taxa distribution modeling.

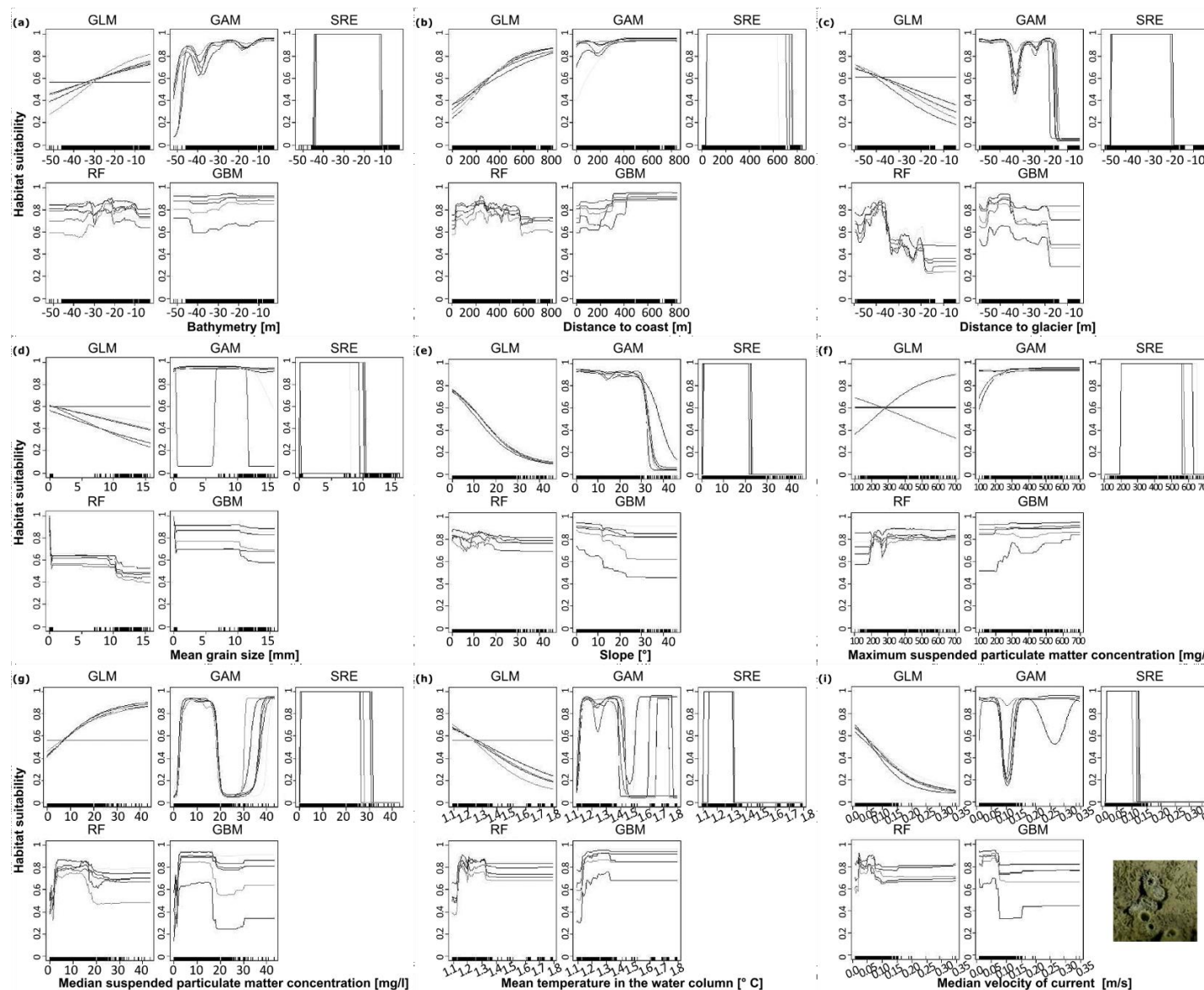


Fig. S6.7. Response curves of habitat suitability (measured as a probability of occurrence from 0 to 1) of *Laternula elliptica* for the nine environmental selected predictors for taxa distribution modeling.

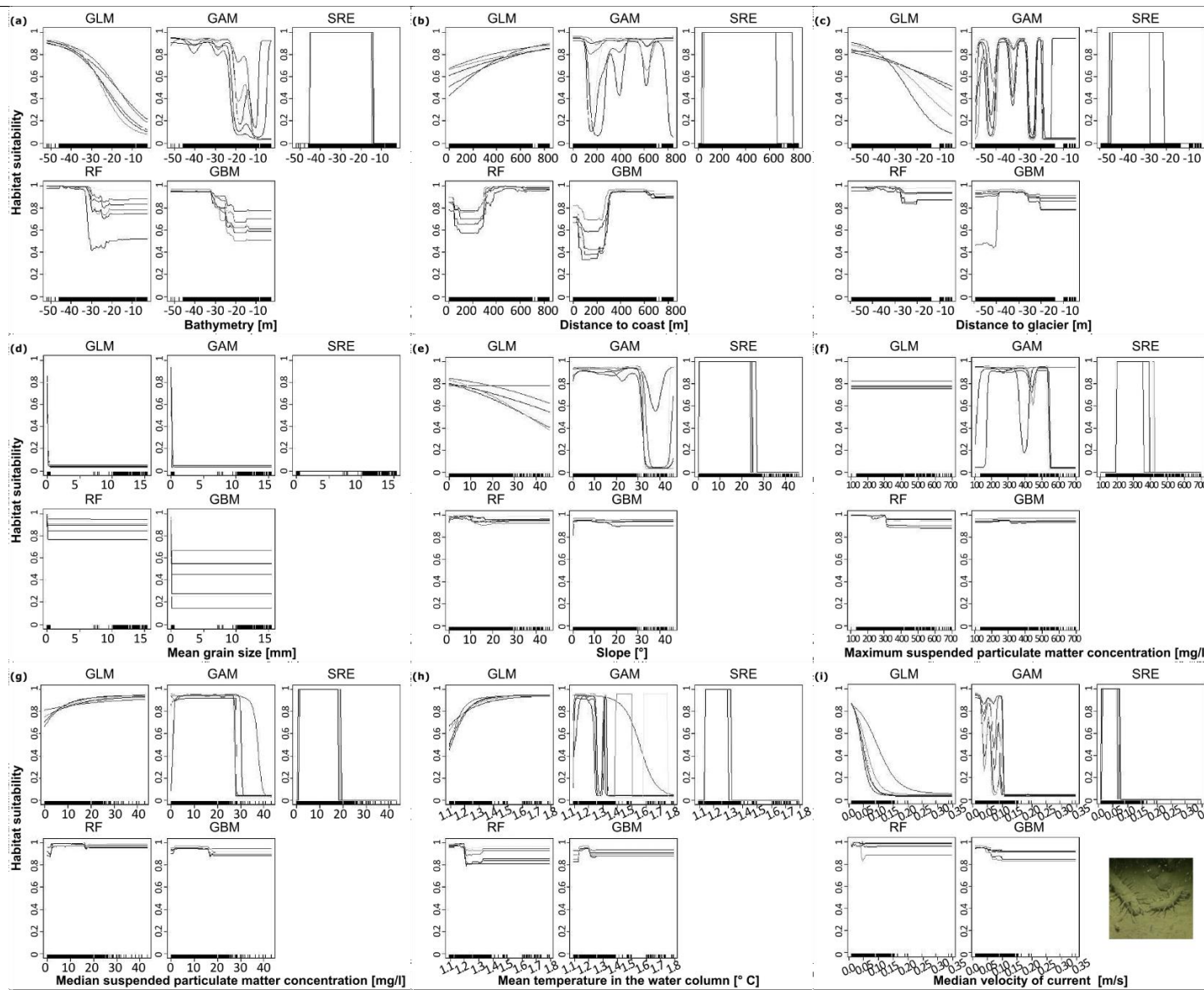


Fig. S6.8. Response curves of habitat suitability (measured as a probability of occurrence from 0 to 1) of *Errantia* for the nine environmental selected predictors for taxa distribution modeling.

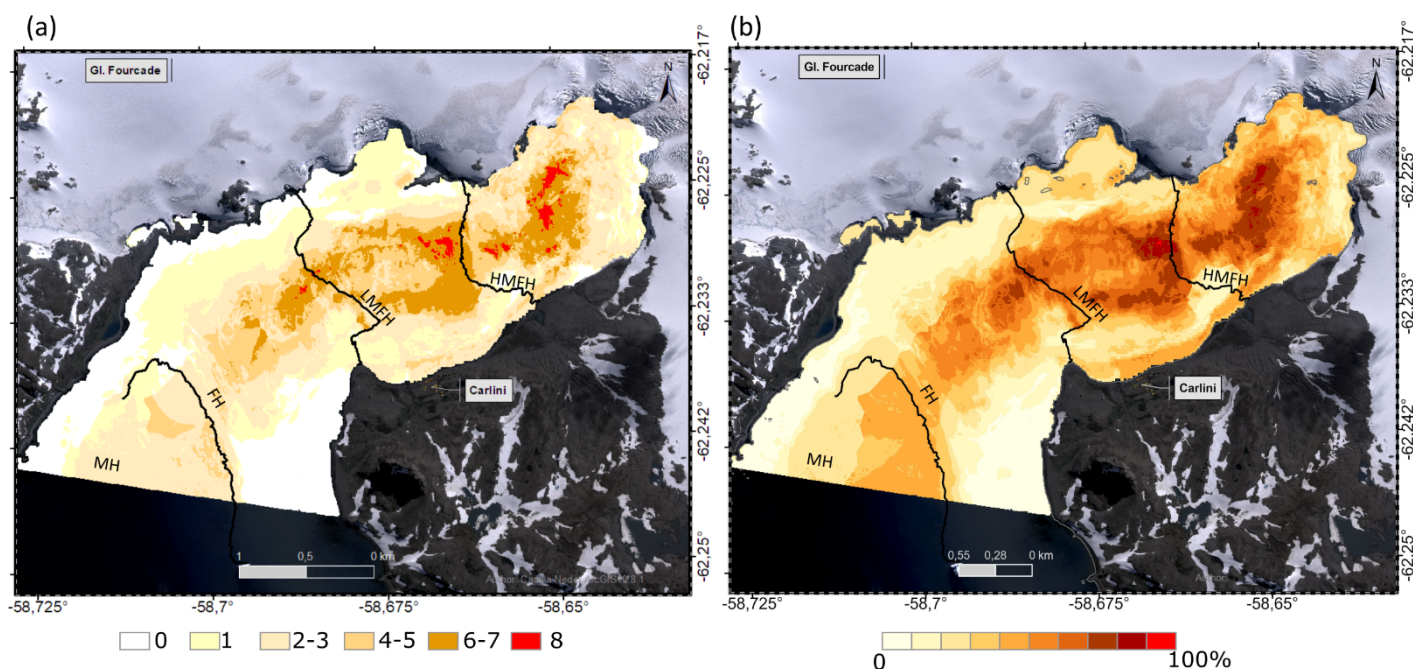


Fig. S7. Compositional analysis results by two different methods. **(a)** Binary transformation was calculated by overlapping the eight taxa-specific binary map results and counting the potential presence (suitable habitat). **(b)** Stacking probabilities by the sum of probability S- SDM (pS-SDM). Values are presented as percentages. Note different scales. Despite the fact of a similar pattern on the location with a high potential co-occurrence the sum of probability informs that there exists a certain probability of co-occurrence of the eight analyzed taxa. Meanwhile, the binary map allows the determination of the number of species predicted to be found in a certain location. This method enables tracking back from single taxa binary conversion in which taxa is involved or even the locations where none of them are potentially present (contrary to pS-SDM where 0% is not identified).

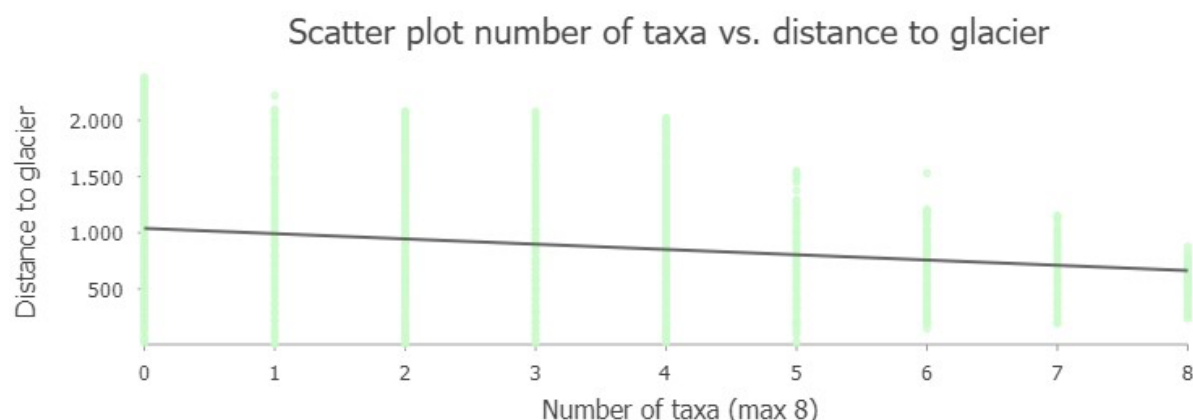


Fig. S8. Scatter plot showing a trend between the distance to the glacier and the number of taxa overlapped. Being the area close to the Fourcade glacier front recently free of ice and available for colonization, despite the trend of an increased co-occurrence close to the glacier front, none of the taxa were exclusively predicted to be present either in recently ice-free or older areas.

LITERATURE CITED

- DigitalGlobe (2014) WorldView-2 103001001F612100, Base Map: scene 07/03/2013, under a CC BY License, with Permission from Maxar-EU Space Imaging-DigitalGlobe.
- Falk U, Gieseke H, Kotzur F, Braun M (2016) Monitoring snow and ice surfaces on King George Island, Antarctic Peninsula, with high resolution TerraSAR-X time series. *Antarct Sci* 28:135–149 <https://doi.org/10.1017/S0954102015000577>
- Falk U, López DA, Silva-Busso A (2018a) Multi-year analysis of distributed glacier mass balance modelling and equilibrium line altitude on King George Island, Antarctic Peninsula. *Cryosphere* 12:1211–1232. <https://doi.org/10.5194/tc-12-1211-2018>
- Falk U, Silva-Busso A (2021) Discharge of groundwater flow to Potter Cove on King George Island, Antarctic Peninsula. *Hydrol Earth Syst Sci* 25:3227–3244. <https://doi.org/10.5194/hess-25-3227-2021>
- Falk U, Silva-Busso A, Pölcher P (2018b) A simplified method to estimate the run-off in Periglacial Creeks: A case study of King George Islands, Antarctic Peninsula. *Philos Trans R Soc A Math Phys Eng Sci* 376:20170166. <https://doi.org/10.1098/rsta.2017.0166>
- Jerosch K, Scharf FK, Deregibus D, Campana GL, Zacher K, Pehlke H, Abele D, Quartino ML (2015) High resolution bathymetric compilation for Potter Cove, WAP, Antarctica, with links to data in ArcGIS format. PANGAEA.
- Marmion M, Parviaainen M, Luoto M, Heikkinen RK, Thuiller W (2009) Evaluation of consensus methods in predictive species distribution modelling. *Divers Distrib* 15:59–69.
- Monien D, Monien P, Brünjes R, et al (2017) Meltwater as a source of potentially bioavailable iron to Antarctica waters. *Antarct Sci* 29:277–291. <https://doi.org/10.1017/S095410201600064X>
- Neder C (2023) El bentos antártico y su respuesta al cambio climático: una aproximación usando modelos de distribución de especies como caso de estudio en caleta Potter. Tesis Doctoral. Universidad Nacional de Córdoba. <http://hdl.handle.net/11086/551476>
- Neder C., & Pehlke, H. (2024). SDM_biomod2 v3.5 for Benthic distribution in an Antarctic fjord area under glacier retreat. <https://doi.org/10.5281/zenodo.14236049>
- Neder C, Fofanova V, Androsov A, et al (2022) Modelling suspended particulate matter dynamics at an Antarctic fjord impacted by glacier melt. *J Mar Syst* 231:103734. <https://doi.org/10.1016/j.jmarsys.2022.103734>
- Neder C, Jerosch K, Monien D, et al (2016a) Suspended particulate matter (SPM) and meteorological data in Potter Cove (74 stations), Carlini Station, King George Island (Isla 25 de Mayo) of 21 years German-Argentinian cooperation (1992–2013) compiled IMCONet. within PANGAEA. <https://doi.org/10.1594/PANGAEA.871275>
- Neder C, Jerosch K, Ruiz Barlett E, Schloss IR (2017) A join of 85 physical oceanography CTD profiles with meteorological variables in Potter Cove, Carlini Station, King George Island (Isla 25 de Mayo) during 24 years German Argentinian cooperation (1991–2015) compiled within IMCONet. PANGAEA. <https://doi.org/10.1594/PANGAEA.870573>
- Sahade R, Lagger C, Momo FR, et al (2015) Climate change, glacier retreat and shifts in an Antarctic benthic ecosystem. 1:e1500050. *Sci Adv* <https://doi.org/10.1126/sciadv.1500050>
- Thuiller W, Georges D, Gueguen M, Engler R, Breiner FT (2021) Biomod2: Ensemble Platform for Species Distribution Modeling. <https://cran.r-project.org/package=biomod2>
- U.S. Geological Survey (2019) Landsat 8 Surface Reflectance Code (LASRC) Product Guide. (No. LSDS-1368 Version 2.0). 40
- Wölfli A-C, Hass HC, Kuhn G (2013) Grain size, TOC, TC, TN, TS and sulphate distribution in surface sediments from Potter Cove, King George Island, Antarctica. PANGAEA. <https://doi.org/10.1594/PANGAEA.815205>
- Wölfli A-C, Lim CH, Hass HC, et al (2014) Distribution and characteristics of marine habitats in a subpolar bay based on hydroacoustics and bed shear stress estimates-Potter Cove, King George Island, Antarctica. *Geo Marine Lett* 34:435–446. <https://doi.org/10.1007/s00367-014-0375-1>